CHALMERS
UNIVERSITY OF TECHNOLOGY

Direct measurement of enthalpy and entropy changes in NH3 promoted O2 activation over Cu−CHA at low temperature

Direct measurement of enthalpy and entropy changes in NH_3 promoted O_2 activation over Cu–CHA at low temperature

Xueting Wang[+],*[a] Lin Chen[+],[b] Peter N. R. Vennestrøm,[c] Ton V. W. Janssens,[c] Jonas Jansson,[d] Henrik Grönbeck,*[b] and Magnus Skoglundh*[a]

Oxygen activation is a key step in the selective catalytic reduction of nitrogen oxides with ammonia (NH_3-SCR) over Cu-chabazite. We present direct measurements of oxygen adsorption at low temperatures over $[NH_3–Cu–NH_3]^+$ complexes and framework-bound Cu^+ species in Cu-chabazite with Si/Al = 14 using isothermal microcalorimetry combined with mass spectrometry. The enthalpy change for O_2 adsorption over $[NH_3–Cu–NH_3]^+$ complexes at 200 °C is determined to be −79 kJ/mol. By fitting a Langmuir isotherm, the corresponding entropy change is determined to be −142 J/(mol*K) at 10% O_2. The results show that O_2 adsorption at low temperatures over $[NH_3–Cu–NH_3]^+$ complexes is more facile than on framework-bound Cu^+ species. The experimental results are in agreement with density functional theory calculations showing a lower barrier for O_2 activation over the $[NH_3–Cu–NH_3]^+$ complexes as compared to the framework-bound Cu^+ species.

Introduction

Copper-functionalised zeolites with the chabazite framework structure (Cu–CHA) are efficient catalysts for selective catalytic reduction of nitrogen oxides (NO_x) by ammonia (NH_3-SCR). This reaction is the basis for the current technology to control NO_x emissions from diesel and bio-diesel exhausts.[1,2] The NH_3-SCR reaction over Cu–CHA has been intensively studied and reaction mechanisms have been proposed with some variations in elementary steps and structural configurations.[3–6] In general, the reaction is based on a redox cycle, where Cu(I) is oxidised by O_2 and reduced by NH_3 and NO.[3,6,7] Furthermore, the reaction mechanism at temperatures below 250 °C has been shown to be different from that at higher temperatures.[8,9] The change in reaction mechanism often leads to a decrease in the NO_x conversion with increasing temperature in the range 250–350 °C. According to the current views of the NH_3-SCR reaction, the change in reaction mechanism is related to a change in the character of the active Cu(I) species. At low temperature, the Cu(I) species are solvated by NH_3-ligands forming mobile $[NH_3–Cu–NH_3]^+$ complexes, whereas Cu(I) species become bound to the framework at higher temperatures.[5,7,9–12] At low temperatures, it has been suggested that O_2 is activated over a pair of $[NH_3–Cu–NH_3]^+$ complexes.[4,5,12,13] This suggestion is based experimentally on the observation that, at low Cu loadings, the NH_3-SCR reaction shows a second order dependence on the Cu loading and that the oxidation of Cu(I) with O_2 has a second order behaviour.[4,9] Moreover, density functional theory (DFT) calculations have revealed that O_2 activation over single framework-bound Cu^+ species is strongly endothermic, whereas O_2 activation becomes feasible if O_2 reacts with a pair of Cu(I)-ions.[12,14,15]

According to the present understanding, the oxidation of Cu(I) with O_2 should be more efficient over the $[NH_3–Cu–NH_3]^+$ complex, as compared to framework-bound Cu^+. In this work, we present a microcalorimetry study of O_2 adsorption on $[NH_3–Cu–NH_3]^+$ complexes and framework-bound Cu^+ species in Cu–CHA, and compare the experimental results with DFT calculations. The measurements allow for direct determination of the enthalpy change upon O_2 adsorption over pairs of $[NH_3–Cu–NH_3]^+$ complexes. By fitting a Langmuir isotherm, the corresponding entropy change can also be determined. By simultaneously monitoring the heat release and the amount of oxygen adsorbed using mass spectrometry, we show that O_2 adsorbs on both types of Cu(I) species at 200 °C. The process is, however, considerably more facile over the $[NH_3–Cu–NH_3]^+$ complexes. The apparent activation energy of O_2 adsorption over the $[NH_3–Cu–NH_3]^+$ complexes is determined to be lower than over the framework-bound Cu^+ species. The experimental results are in agreement with the DFT calculations showing a lower

[a] X. Wang,[+] M. Skoglundh
Department of Chemistry and Chemical Engineering and Competence Centre for Catalysis, Chalmers University of Technology, Gothenburg, 412 96, Sweden
E-mail: xueting.wang@chalmers.se
skoglund@chalmers.se
[b] L. Chen,[+] H. Grönbeck
Department of Physics and Competence Centre for Catalysis, Chalmers University of Technology, Gothenburg, 412 96, Sweden
E-mail: ghj@chalmers.se
[c] P. N. R. Vennestrøm, T. V. W. Janssens
Umicore Denmark ApS, Kogle Allé 1, 2970 Hørsholm, Denmark
[d] J. Jansson
Volvo Group Trucks Technology, Gothenburg, 405 08, Sweden
[+] Contributed equally to this work

Supporting information for this article is available on the WWW under https://doi.org/10.1002/cctc.202100253

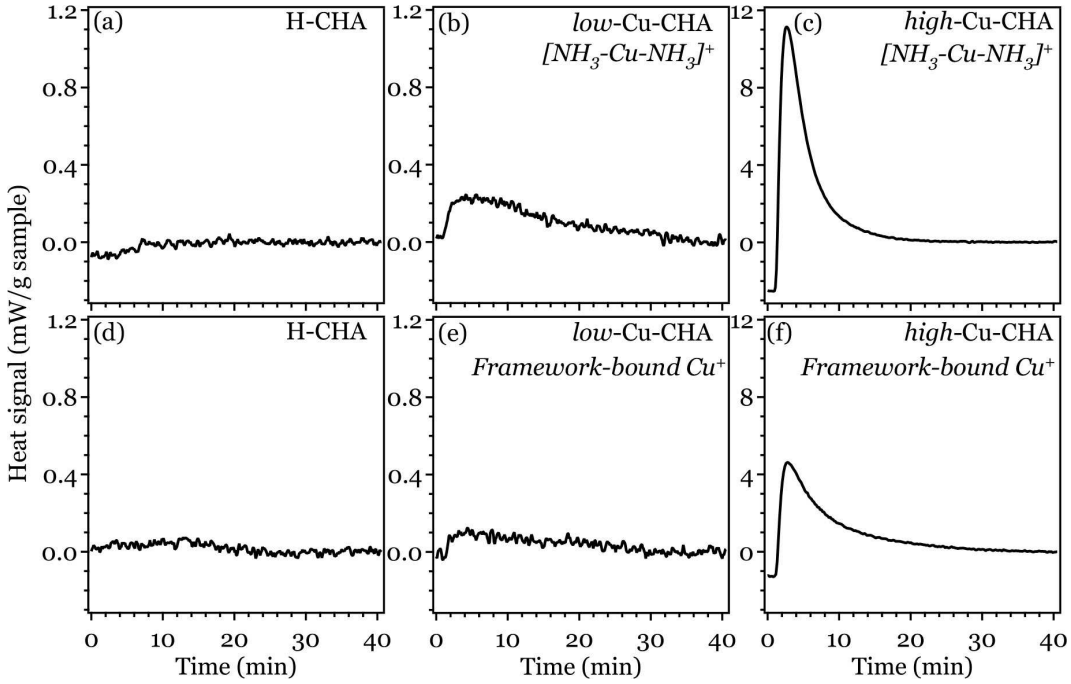

Figure 1. Heat signal recorded during O_2 exposure (500 ppm) at 200 °C over the H–CHA, *low*- and *high*–Cu–CHA samples. (a-c) are pre-treated in NO and NH_3 at 200 °C (see SI, S1.2) yielding $[NH_3–Cu–NH_3]^+$ complexes for (b) and (c). (d-f) are subsequently pre-treated in O_2 at 500 °C (see SI, S1.2) yielding framework-bound Cu^+ species for (e) and (f). Note that the range of the y-axis for the *high*–Cu–CHA sample is a magnitude higher than that of the other samples.

barrier for O_2 activation over the $[NH_3–Cu–NH_3]^+$ complexes as compared to the framework-bound Cu^+ species.

Experimental

Two aqueous ion-exchanged Cu–CHA (Si/Al = 14) samples with low and high copper loading were prepared, *i.e.* *low*–Cu–CHA (0.60 wt.% Cu) and *high*–Cu–CHA (3.3 wt.% Cu) (see SI, S1.1). The parent H–CHA zeolite was used as reference. To form the $[NH_3–Cu–NH_3]^+$ complexes, the Cu–CHA samples were reduced in NO and NH_3 at 250 °C for 30 min and subsequently at 200 °C for 30 min.[8,16] The framework-bound Cu^+ species were formed by heating the reduced sample in Ar to 500 °C for 60 min whereby the $[NH_3–Cu–NH_3]^+$ complexes decompose yielding predominantly framework-bound Cu^+ species (see SI, S1.2).[8,17] The $[NH_3–Cu–NH_3]^+$ complexes and the framework-bound Cu^+ species have been identified using X-ray absorption spectroscopy in previous studies in Cu–CHA samples with similar Si/Al ratio and Cu loadings.[8,16,17] The heat signal during exposure of the $[NH_3–Cu–NH_3]^+$ complexes and the framework-bound Cu^+ species in a gas flow containing 500 ppm of O_2 in Ar at 200 °C was recorded for the two Cu–CHA samples and the parent H–CHA zeolite, using a flow-through sample cell for the calorimetry. The amount of adsorbed oxygen was determined from the difference of m/Z = 32, and the scaled m/Z = 84 intensity of Kr as trace gas, using a mass spectrometer connected to the outlet of the sample cell.

Results and Discussion

Figure 1 shows the heat release during O_2 adsorption for the parent zeolite, and for the NH_3 solvated and framework-bound Cu(I) in the two Cu–CHA catalysts. The corresponding heat release, calculated heat of adsorption and O/Cu ratio are presented in Table 1. No significant heat release is observed during O_2 exposure of the H–CHA zeolite at 200 °C, while there are clear heat effects for the Cu–CHA samples. For the samples with the $[NH_3–Cu–NH_3]^+$ complexes, we find a heat release of 0.23 J/g for the *low*–Cu–CHA sample, and a significantly higher release of 3.2 J/g for the *high*–Cu–CHA sample. The corresponding numbers for the samples with framework-bound Cu^+ species are 0.09 J/g for the *low*–Cu–CHA sample and 2.1 J/g for the *high*–Cu–CHA sample. The two important observations are (1) the heat release for the catalysts with the $[NH_3–Cu–NH_3]^+$ complexes is higher than the heat release for the framework-bound Cu^+ species, and (2) the heat release for the *high*–Cu–CHA sample is considerably higher than for the *low*–Cu–CHA sample.

Figure 2 presents the heat release during O_2 exposure over the $[NH_3–Cu–NH_3]^+$ complexes and the framework-bound Cu^+ species in the *high*–Cu–CHA sample between 75 to 275 °C. For the $[NH_3–Cu–NH_3]^+$ complexes, the heat release increases with increasing temperature up to 200 °C after which it substantially decreases. Below 200 °C, we speculate that the possibility to activate O_2 over Cu(I)-pairs increases with increasing temperature thanks to faster diffusion of the $[NH_3–Cu–NH_3]^+$ complexes, resulting in an increased heat release. It is known that $[NH_3–Cu–NH_3]^+$ starts to decompose above 200 °C, yielding framework-bound $[Cu\text{-}NH_3]^+$ and Cu^+ species.[8,18] It is anticipated that the sharp decrease in heat release for temperatures above 200 °C is a result of decomposition of the $[NH_3–Cu–NH_3]^+$ complexes. For the framework-bound Cu^+ species, the heat release instead increases within the entire temperature range examined. No

Table 1. Heat release, heat of oxygen adsorption and O/Cu ratio measured during O_2 exposure (500 ppm) at 200 °C over H–CHA and Cu–CHA with either $[NH_3–Cu–NH_3]^+$ complexes or framework-bound Cu^+ species at low and high Cu-loadings. The samples are pre-treated as in Figure 1.

		H–CHA	*low*–Cu–CHA	*high*–Cu–CHA[a]
$[NH_3–Cu–NH_3]^+$	J/g sample	0.00	0.23	3.2 ± 0.1
	kJ/mol Cu	n.a.	2.5	6.2 ± 0.3
	kJ/mol O_2	n.a.	n.a.	79 ± 6
	O/Cu[b]	n.a.	n.a.	0.16 ± 0.01
Framework-bound Cu^+	J/g sample	0.04	0.09	2.1 ± 0.3
	kJ/mol Cu	n.a.	1.0	4.0 ± 0.5
	kJ/mol O_2	n.a.	n.a.	120 ± 9
	O/Cu[b]	n.a.	n.a.	0.07 ± 0.01

[a] The values are averaged from three separate measurements for each Cu species, see SI, S3.1. [b] The O/Cu ratio is calculated by dividing double the amount of adsorbed O_2 [mol/g catalyst], by the total amount of Cu [mol/g catalyst].

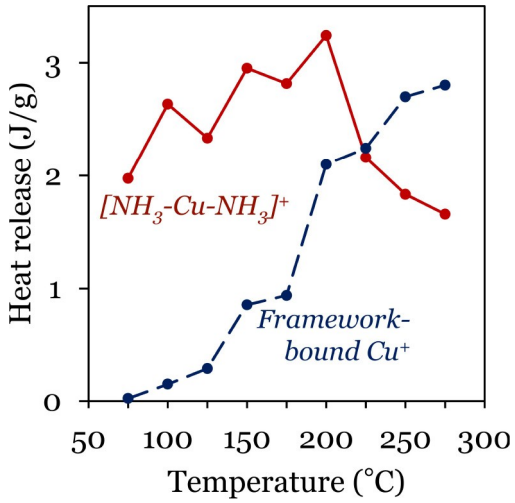

Figure 2. Heat release during O_2 exposure (500 ppm) over the $[NH_3–Cu–NH_3]^+$ complexes (red dots with solid line for guidance) and the framework-bound Cu^+ species (blue dots with dashed line for guidance) in the *high*–Cu–CHA sample between 75 and 275 °C.

significant heat release is in this case observed below 150 °C. From the O_2 exposure experiments the apparent activation energies were obtained. The activation enthalpy for O_2 adsorption over $[NH_3–Cu–NH_3]^+$ complexes and framework-bound Cu^+ species is determined to be 15 and 39 kJ/mol, respectively (see SI, S3.2).

The measured heats of O_2 adsorption on the different Cu(I) species are compared with DFT calculations. Figure 3 shows possible reaction paths for the O_2 adsorption over the $[NH_3–Cu–NH_3]^+$-pairs and framework-bound Cu^+-pairs. The CHA structure is modelled using a hexagonal unit cell, which includes 36 tetrahedral positions with two Al atoms per unit cell, corresponding to an Si/Al ratio of 17. Because it is unlikely to have Al–O–Si–O–Al sequences in Si-rich zeolites,[19] we use an Al–O-(Si–O)$_2$-Al sequence with two Al atoms placed in neighbouring six-membered rings to describe the general trends. In our previous work,[14] the Al-distribution has been found to have an effect on the stability of the $[NH_3–Cu–NH_3]^+$-pairs in Cu–CHA, which probably will affect the probability for $[NH_3–Cu–NH_3]^+$-pair formation. The dependence of the O_2 adsorption energy on the Al-distribution is studied by considering five different structural configurations. The five configurations are selected from our previous work,[14] and corresponds to an Al–Al distance of 6.28, 7.24, 8.60, 11.46 and 13.77 Å, respectively. Further details of the calculations are given in SI, S2.

To directly compare the experimentally measured heats of O_2 adsorption with the calculated values, the reference (zero level) for the O_2 adsorption over the $[NH_3–Cu–NH_3]^+$-pair is considered to be the precursor state of the molecularly adsorbed O_2 (see the structure Cu-pair in Figure 3(a)). In similarity, the reference for the O_2 adsorption over the framework-bound Cu^+-pairs is taken when the two Cu ions are close enough for O_2 to adsorb (see the structure Cu-pair in Figure 3(b)). The final structure for the adsorption of O_2 in a peroxo-state has been studied in detail in Refs. [6, 16, 20].

Previously, the linear $[NH_3–Cu–NH_3]^+$ complex has been shown to be mobile at reaction temperatures[7] and the diffusion barrier between cages is calculated to be low (~0.3 eV).[21] Thus, the diffusion step has not been considered in this reaction mechanism (Figure 3(a)). The adsorption of O_2 over the complex-pair proceeds via molecular O_2 adsorption (CuO_2Cu) to the peroxo-state (CuOO–Cu) with a low barrier of 21 kJ/mol. The final CuOOCu configuration is a singlet with two antiferromagnetically coupled magnetic moments (0.6 μ_B per copper ion), implying that the formal oxidation state of copper in this configuration is +2.[20] The five different Al-distribution configurations give a span of the adsorption enthalpy of O_2, which ranges from 53 to 71 kJ/mol. The difference between the configurations originates mainly from the different Coulomb interactions among the five configurations.

The adsorption of O_2 over the framework-bound Cu^+ also requires a pair of Cu^+ ions, which has been discussed in Ref. [15]. A possible reaction path for O_2 activation over the framework-bound Cu^+-pair is shown in Figure 3(b). Here, the locations of the two Al atoms are similar with that used in Ref. [15]. Each Cu^+ species is preferably located in the six-membered ring bridging two framework oxygen atoms (2Cu).[21–23] To make it feasible to adsorb O_2, the two Cu^+ ions need to be sufficiently close. The barrier for Cu^+ ion diffusion forming the Cu-pair structure is calculated to be 72 kJ/mol and the pair formation is endothermic by 38 kJ/mol. The activation of O_2 over the framework-bound Cu ions from this configuration (Cu-pair) has a low barrier of 19 kJ/mol. The final

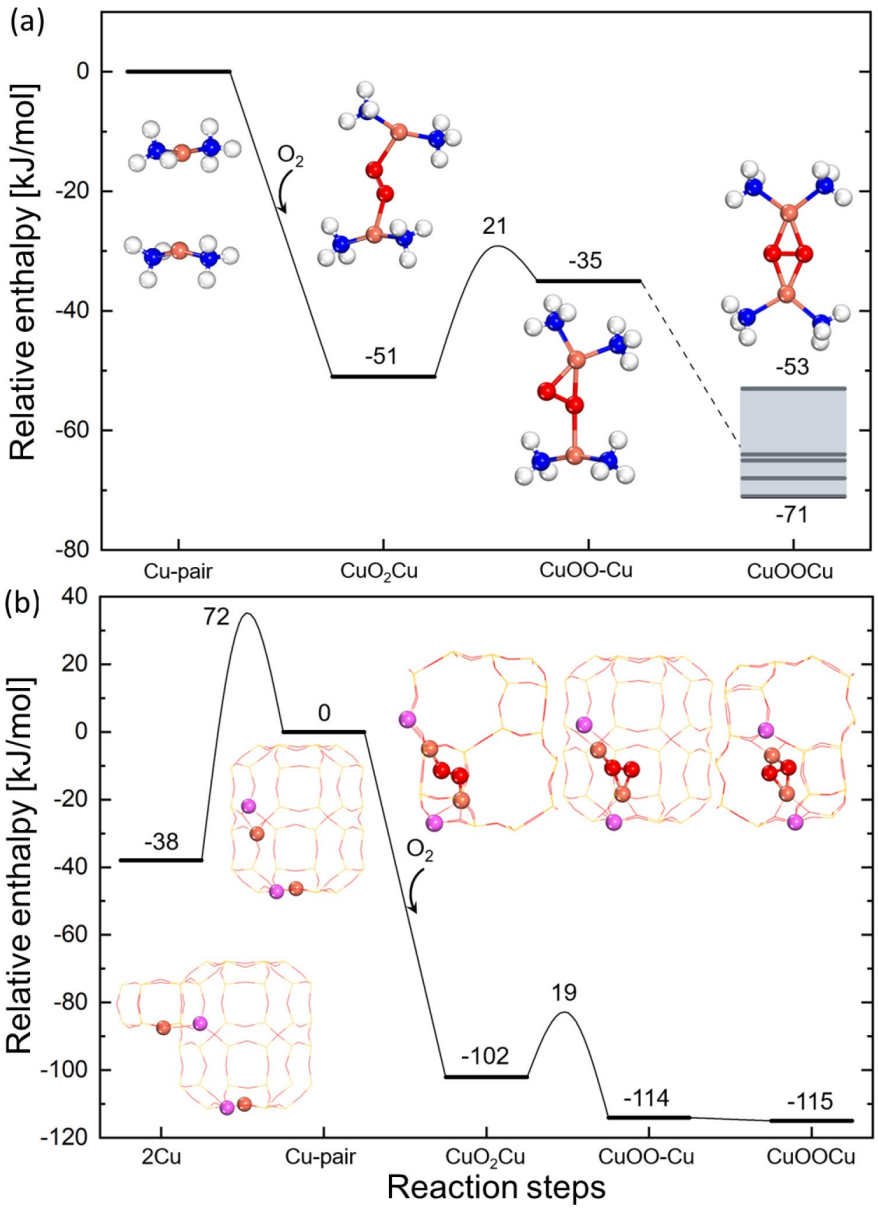

Figure 3. The potential enthalpy landscape at 200 °C of: (a) O_2 adsorption over $[NH_3–Cu–NH_3]^+$-pairs in Cu–CHA; (b) O_2 adsorption over framework-bound Cu^+-pairs. Five selected different Al-distribution configurations for the mobile Cu-complex pair case have been chosen to study the dependence of adsorption energies on the Al-distribution, which results in a span of adsorption enthalpy. The structure for each step is shown. For clarity, the CHA framework is removed in (a) and kept as lines in (b). All energies are zero-point corrected. Atom colour codes: copper (light brown), aluminium (purple), nitrogen (blue), oxygen (red) and hydrogen (white).

CuOOCu species is a triplet with magnetic moments on the copper ions for which we assign the formal oxidation state of copper to be +2. The total adsorption energy for the activated O_2 over the framework-bound Cu^+-pair is 115 kJ/mol.

The DFT results are in good agreement with the micro-calorimetry data, showing a lower barrier over $[NH_3–Cu–NH_3]^+$ complexes as compared to framework-bound Cu^+ species. The barrier for O_2 adsorption is calculated to be 21 kJ/mol over the $[NH_3–Cu–NH_3]^+$ pair, which is close to our experimental value of 15 kJ/mol determined from the Eyring plot (SI S3.2). The corresponding barriers are not as close for the framework-bound case (72 vs 39 kJ/mol), which can be attributed to the choice of Al-distribution. The DFT calculations show that the origin of the apparent activation energy is different for the two cases. The barrier for O_2 activation over the $[NH_3–Cu–NH_3]^+$ pair originates from the formation of the CuOO–Cu species, whereas the barrier over framework-bound Cu^+ is connected with diffusion of Cu^+ ions, forming a Cu^+-pair.

From the DFT calculations, the adsorption enthalpy of activated O_2 over the $[NH_3–Cu–NH_3]^+$-pairs is within a range (from 53 to 71 kJ/mol), which is slightly lower than the measured heat (79 kJ/mol). Possible reasons for the discrepancy in the absolute energies can be related to the Al-distribution as well as the difficulty to accurately describe the Cu–O bond by

the current exchange correlational functional.[20] However, our DFT results predict the trend in a good agreement with the measured heat of adsorption, which shows a lower heat of adsorption for the $[NH_3–Cu–NH_3]^+$ complexes (79 kJ/mol) compared to that of the framework-bound Cu^+ species (120 kJ/mol) for the *high*–Cu–CHA sample.

The calorimetric measurements at 200 °C show that the heat release is higher for the $[NH_3–Cu–NH_3]^+$ complexes than for the framework-bound Cu^+ species regardless of Cu loading. The difference in heat release is related to a higher amount of oxygen adsorbed on the $[NH_3–Cu–NH_3]^+$ complexes compared to the framework-bound Cu^+ species (see SI, S3.1). As the direct O_2 activation requires Cu(I)-pairs for both framework bound and NH_3-solvated copper species, this implies that the propensity for pair formation is higher for $[NH_3–Cu–NH_3]^+$ complexes than for framework-bound Cu^+ species. This supports the idea that pair formation is facilitated by the higher mobility of the $[NH_3–Cu–NH_3]^+$ complexes.[7,21,24] For framework-bound Cu^+ species, pair-formation is associated with a barrier of 72 kJ/mol originating from Cu^+ diffusion between adjacent cages (Figure 3(b)), rendering Cu^+-pair formation less probable. Therefore, the higher heat release for the $[NH_3–Cu–NH_3]^+$ complexes is related to the higher mobility, providing more sites for O_2 activation.

The higher propensity of O_2 adsorption on the $[NH_3–Cu–NH_3]^+$ complexes is also reflected in the higher amount of oxygen adsorbed. Assuming that oxygen only adsorbs over Cu(I)-pairs, for the *high*–Cu–CHA sample with pre-treatment to form dominantly $[NH_3–Cu–NH_3]^+$ complexes, around 16% of the total Cu content is oxidised during exposure to 500 ppm O_2 at 200 °C, whereas the corresponding number is about 7% for the pre-treatment forming dominantly framework-bound Cu^+ species, see Table 1. Moreover, the fraction of copper participating in O_2 adsorption varies for the two Cu–CHA samples, which is indicated by the heat release per Cu (shown in Table 1). The heat-release per Cu ($[NH_3–Cu–NH_3]^+$ or framework-bound Cu^+) is higher for the *high*–Cu–CHA sample (6.2 and 4.0 kJ/mol Cu) compared to the *low*–Cu–CHA sample (2.5 and 1.0 kJ/mol Cu). This suggest that sufficiently high Cu-density is required for Cu(I) pair formation and thereby O_2 adsorption, which is in agreement with previous studies.[4,12,15]

The heat released during O_2 exposure over the $[NH_3–Cu–NH_3]^+$ complexes is also affected by the O_2 concentration. Figure 4 presents heat release as a function of oxygen concentration from 500 ppm to 12%. Assuming the same mechanism and, therefore, heat of oxygen adsorption for all tested O_2 concentrations, the O/Cu ratio can be calculated for each O_2 concentration, as also presented in Figure 4. For exposure at 10% O_2, the calculated O/Cu ratio is 0.8 which is comparable to the 80–90% of Cu(II) oxidised from Cu(I) observed spectroscopically in previous studies over similar Cu–CHA samples.[4,16] The experimental data can be fitted with a Langmuir isotherm:

$$\theta = \mathrm{O/Cu} = \frac{a K^{\circ}_{eq}(T)\frac{po_2}{p^{\circ}}}{1 + K^{\circ}_{eq}(T)\frac{po_2}{p^{\circ}}} = \frac{0.848 \times 207 \times \frac{po_2}{p^{\circ}}}{1 + 207 \times \frac{po_2}{p^{\circ}}},\ R^2 = 0.979 \quad (1)$$

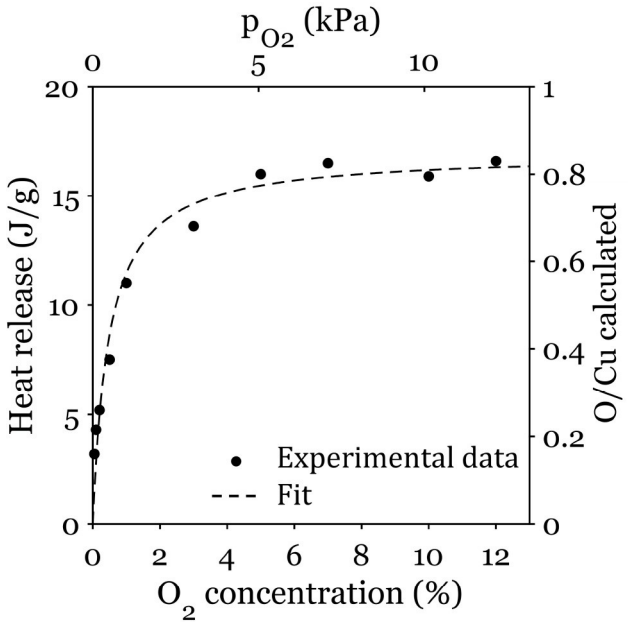

Figure 4. Heat release and O/Cu ratio during exposure of the $[NH_3–Cu–NH_3]^+$ complexes to O_2 from 500 ppm to 12% at 200 °C. The O/Cu ratio for O_2 concentrations (c_{O_2}) higher than 500 ppm is calculated using data measured at $c_{O_2} = 500$ ppm, assuming constant heat of adsorption under all c_{O_2}. The corresponding partial pressure of O_2 (p_{O_2}) is shown at the top axis.

where θ is the coverage and $K^{\circ}_{eq}(T)$ is the equilibrium constant at standard pressure (P °). The constant *a* limits the coverage to the experimentally observed saturation coverage. The $K^{\circ}_{eq}(T)$ and *a* is fitted to be 207 and 0.848 at 200 °C, respectively.

The entropy change for reactions in zeolites has been discussed recently in the literature. For the NH_3-SCR reaction some estimates for entropy changes along the reaction path have been suggested based on simulations.[5,6,16] However, no quantitative experimental data has been reported. The information on the equilibrium constant and the heat of adsorption gives us the possibility to calculate the entropy loss for O_2 adsorption over the $[NH_3–Cu–NH_3]^+$-pair. The equilibrium constant is given by:[25]

$$K^{\circ}_{eq}(T) \times \frac{po_2}{p^{\circ}} = \exp\left(-\frac{\Delta G}{RT}\right) = \exp\left(-\frac{\Delta H}{RT}\right)\exp\left(\frac{\Delta S}{R}\right) \quad (2)$$

where ΔH is the enthalpy change and ΔS is the entropy change. Using the experimentally determined ΔH, the entropy change ΔS is via the equilibrium constant calculated to be -123 J/(mol*K) at standard pressure. Typically, the O_2 concentration during NH_3-SCR is 10%, which gives an entropy change of -142 J/(mol*K).

The entropy change of O_2 adsorption on a pair of complexes has three main contributions (see the schematic diagram in Figure S4 in SI). Upon entering the CHA cage from the gas phase, O_2 loses entropy. Previously, we have studied the entropy loss for N_2 from gas phase into CHA by performing Monte Carlo potential energy sampling,[26] which demonstrates

that N_2 loses approximately 50% of the gas phase entropy at 200 °C. Here, we can assume that O_2 also loses 50% of its gas phase entropy upon entering CHA ($\Delta S^1_{O_2} = -109$ J/(mol*K)). Another part of the O_2 entropy ($\Delta S^2_{O_2}$) is lost upon adsorption over the $[NH_3–Cu–NH_3]^+$-pair. In addition, there is an entropy loss connected to the pairing of the complexes (ΔS_{Cu}). Here, the sum of the three contributions is fitted to be −123 J/(mol*K) at standard pressure. The sum of $\Delta S^2_{O_2}$ and ΔS_{Cu} amounts to −14 J/mol*K, which is a minor part of the entropy loss.

Conclusion

In summary, we have compared the heat of O_2 adsorption over $[NH_3–Cu–NH_3]^+$ complexes and framework-bound Cu^+ species in CHA as measured by microcalorimetry combined with mass spectrometry and compared the results with DFT calculations. For O_2 adsorption over $[NH_3–Cu–NH_3]^+$ complexes at 200 °C, the heat of adsorption is 79 kJ/mol while the entropy change is analysed to be −142 J/mol*K at 10% O_2. The results reveal that a higher amount of O_2 adsorbs over the $[NH_3–Cu–NH_3]^+$ complexes than over the framework-bound Cu^+ species at 200 °C. The DFT calculations show that the activation of O_2 proceeds with low barriers over both types of Cu-pairs. However, the diffusion of framework-bound Cu^+ species between adjacent CHA cages is associated with considerable barriers, which makes the Cu^+-pair formation less facile. The low probability of Cu^+-pair formation for framework-bound Cu–CHA consequently leads to a lower O_2 adsorption upon O_2 exposure as compared to the $[NH_3–Cu–NH_3]^+$ complexes. The higher amount of O_2 adsorbed on $[NH_3–Cu–NH_3]^+$ complexes as compared to framework-bonded Cu^+ species, provides further support for the suggestion that the mobility of the $[NH_3–Cu–NH_3]^+$ complexes is a key factor for the activation of O_2 in low-temperature NH_3-SCR over Cu–CHA. Furthermore, the observed differences in O_2 activation on the $[NH_3–Cu–NH_3]^+$ complexes and framework-bound Cu^+ species contribute to an enhanced understanding of the underlying chemistry of partial oxidation reactions, such as that of direct oxidation of methane to methanol.

Acknowledgement

This work is financially supported by the Swedish Research Council (2016-5234 and 2017-04811), the Swedish Energy Agency (47110-1), as well as the Competence Centre for Catalysis which is financially supported by Chalmers University of Technology, the Swedish Energy Agency and the member companies: AB Volvo, ECAPS AB, Johnson Matthey AB, Preem AB, Scania CV AB, Umicore Denmark ApS and Volvo Car Corporation AB. The calculations were performed at C3SE (Göteborg) via a SNIC grant.

Conflict of Interest

The authors declare no conflict of interest.

Keywords: adsorption · Cu-chabazite · NH_3-SCR · oxygen activation · zeolites

[1] E. Borfecchia, P. Beato, S. Svelle, U. Olsbye, C. Lamberti, S. Bordiga, *Chem. Soc. Rev.* **2018**, *47*, 8097–8133.
[2] J. Wang, H. Zhao, G. Haller, Y. Li, *Appl. Catal. B* **2017**, *202*, 346–354.
[3] T. V. W. Janssens, H. Falsig, L. F. Lundegaard, P. N. R. Vennestrøm, S. B. Rasmussen, P. G. Moses, F. Giordanino, E. Borfecchia, K. A. Lomachenko, C. Lamberti, S. Bordiga, A. Godiksen, S. Mossin, P. Beato, *ACS Catal.* **2015**, *5*, 2832–2845.
[4] C. Paolucci, I. Khurana, A. A. Parekh, S. Li, A. J. Shih, H. Li, J. R. Di Iorio, J. D. Albarracin-Caballero, A. Yezerets, J. T. Miller, W. N. Delgass, F. H. Ribeiro, W. F. Schneider, R. Gounder, *Science* **2017**, *357*, 898–903.
[5] F. Gao, D. Mei, Y. Wang, J. Szanyi, C. H. F. Peden, *J. Am. Chem. Soc.* **2017**, *139*, 4935–4942, PMID: 28288511.
[6] L. Chen, T. Janssens, P. Vennestrøm, J. Jansson, M. Skoglundh, H. Grönbeck, *ACS Catal.* **2020**, *10*, 5646–5656.
[7] C. Paolucci, A. A. Parekh, I. Khurana, J. R. Di Iorio, H. Li, J. D. Albarracin Caballero, A. J. Shih, T. Anggara, W. N. Delgass, J. T. Miller, F. H. Ribeiro, R. Gounder, W. F. Schneider, *J. Am. Chem. Soc.* **2016**, *138*, 6028–6048, PMID: 27070199.
[8] E. Borfecchia, C. Negri, K. A. Lomachenko, C. Lamberti, T. V. W. Janssens, G. Berlier, *React. Chem. Eng.* **2019**, *4*, 1067–1080.
[9] F. Gao, E. D. Walter, M. Kollar, Y. Wang, J. Szanyi, C. H. Peden, *J. Catal.* **2014**, *319*, 1–14.
[10] K. A. Lomachenko, E. Borfecchia, C. Negri, G. Berlier, C. Lamberti, P. Beato, H. Falsig, S. Bordiga, *J. Am. Chem. Soc.* **2016**, *138*, 12025–12028, PMID: 27532483.
[11] F. Giordanino, E. Borfecchia, K. A. Lomachenko, A. Lazzarini, G. Agostini, E. Gallo, A. V. Soldatov, P. Beato, S. Bordiga, C. Lamberti, *J. Phys. Chem. Lett.* **2014**, *5*, 1552–1559, PMID: 26270095.
[12] L. Chen, H. Falsig, T. V. Janssens, H. Grönbeck, *J. Catal.* **2018**, *358*, 179–186.
[13] A. Marberger, A. W. Petrov, P. Steiger, M. Elsener, O. Krcher, M. Nachtegaal, D. Ferri, *Nat. Catal.* **2018**, *1*, 221–227.
[14] L. Chen, H. Falsig, T. V. W. Janssens, J. Jansson, M. Skoglundh, H. Grönbeck, *Catal. Sci. Technol.* **2018**, *8*, 2131–2136.
[15] H. Falsig, P. N. R. Vennestrøm, P. G. Moses, T. V. W. Janssens, *Top. Catal.* **2016**, *59*, 861–865.
[16] C. Negri, T. Selleri, E. Borfecchia, A. Martini, K. A. Lomachenko, T. V. W. Janssens, M. Cutini, S. Bordiga, G. Berlier, *J. Am. Chem. Soc.* **2020**, *142*, 15884–15896, PMID: 32830975.
[17] A. Martini, E. Borfecchia, K. A. Lomachenko, I. A. Pankin, C. Negri, G. Berlier, P. Beato, H. Falsig, S. Bordiga, C. Lamberti, *Chem. Sci.* **2017**, *8*, 6836–6851.
[18] L. Chen, T. V. W. Janssens, M. Skoglundh, H. Grönbeck, *Top. Catal.* **2019**, *62*, 93–99.
[19] K. Mlekodaj, J. Dedecek, V. Pashkova, E. Tabor, P. Klein, M. Urbanova, R. Karcz, P. Sazama, S. Whittleton, H. Thomas, A. Fishchuk, *J. Phys. Chem. C* **2018**, *123*, 7968–7987.
[20] L. Chen, T. Janssens, H. Grönbeck, *Phys. Chem. Chem. Phys.* **2019**, *21*, 10923–10930.
[21] L. Chen, J. Jansson, M. Skoglundh, H. Grönbeck, *J. Phys. Chem. C* **2016**, *120*, 29182–29189.
[22] F. Göltl, R. Bulo, J. Hafner, P. Sautet, *J. Phys. Chem. Lett.* **2013**, *4*, 2244–2249.
[23] U. Deka, A. Juhin, E. Eilertsen, H. Emerich, M. Green, S. Korhonen, B. Weckhuysen, A. Beale, *J. Phys. Chem. C* **2012**, *116*, 4809–4818.
[24] S. Shwan, M. Skoglundh, L. Lundegaard, R. Tiruvalam, T. Janssens, A. Carlsson, P. Vennestrøm, *ACS Catal.* **2014**, *5*, 16–19.
[25] I. Chorkendorff, J. W. Niemantsverdriet, *Concepts of modern catalysis and kinetics*; John Wiley & Sons, **2017**, p 30.
[26] M. Jørgensen, L. Chen, H. Grönbeck, *J. Phys. Chem. C* **2018**, *122*, 20351–20357.

Manuscript received: February 16, 2021
Revised manuscript received: March 4, 2021
Accepted manuscript online: March 4, 2021
Version of record online: ■■, ■■■

FULL PAPERS